3D cell culture stimulates the secretion of in vivo like exosomes

Sirisha Thippabhotla[1], Lanjing Wei[2], Cuncong Zhong[1,2], Mei He[2,3,4*]

1. Department of Electrical Engineering and Computer Science, University of Kansas, Lawrence, Kansas 66045, USA
2. Bioengineering Research Center, University of Kansas, Lawrence, Kansas 66045, USA
3. Department of Chemical and Petroleum Engineering, University of Kansas, Lawrence, Kansas 66045, USA
4. Department of Chemistry, University of Kansas, Lawrence, Kansas 66045, USA

* meih@ku.edu

ABSTRACT

For studying cellular communications ex-vivo, two-dimensional (2D) cell culture model currently is widely used as the "golden standard", such as, examining exosome RNA expression profiles from tumor cells and tumor biomarker discovery. Although the 2D culture system is simple and easily accessible, the culture environment is unable to represent the in vivo extracellular matrix (ECM) microenvironment. Our study observed that 2D culture derived exosomes showed significantly different profiles in terms of secretion dynamics and essential signaling molecular contents (RNAs and DNAs), compared to the 3D culture derived exosomes. By using the next-generation sequencing of cervical cancer cells and cervical cancer patient plasma-derived exosomal RNA, we observed that 3D culture derived exosomal RNAs may undergo specific sorting process and differ from their parent cells. Most importantly, the 3D culture derived exosomal RNA profile exhibited a much higher similarity (~96%) to in vivo circulating exosomes from cervical cancer patient plasma. However, 2D culture derived exosomal RNA profile is irrelevant and only correlated to their parent cells cultured in 2D. On the other hand, DNA sequencing analysis suggests that culture and growth conditions do not affect the genomic information carried by exosome secretion. This work also suggest that tackling exosomal molecular contents and alterations secreted into interstitial fluids can provide an alternative, non-invasive approach for investigating 3D tissue behaviors at the molecular precision. This work could serve as a foundation for building precise model employed in mimicking in vivo tissue system with exosomes as the molecular vehicle for investigating tumor biomarkers, drug screening, and understanding tumor progression and metastasis.

Introduction

Nearly all living cells secret extracellular vesicles, including mammalian cells, bacteria (named as outer membrane vesicles), fungi and eukaryotic parasites[1]. The first description regarding the presence of vesicles around cells in mammalian tissues or fluids is published in late 1960[2, 3]. However, such cellular secreted vesicles were considered as the "waste bag" at the beginning[4]. Until 2011, the term of extracellular vesicles (EVs) was proposed to define all lipid bilayer-enclosed extracellular structures[5]. Extracellular vesicles (EVs) are a heterogeneous mixture of membranous structures, derived from either the cellular endosomal pathway or shed from the plasma membrane[6]. Due to the different biogenesis, EVs are generally classified as the exosomes (~30-150 nm) and microvesicles (~100-1000nm)[7-10]. Microvesicles with particle size up to 1 μm are formed by the outward budding from the cell membrane [6, 11]. In contrast, exosomes are one subgroup of EVs formed from the intercellular structure via the inward invagination of endosome membranes [12], which encapsulated complex cellular signaling components, including proteins, lipids, and nucleic acids (e.g., mRNA, miRNA, DNA)[13, 14]. Exosomes play important roles in cell-to-cell communications via cross-transferring of important signaling components[15-18]. For instance, exosomes can carry and transmit mRNAs and miRNAs for promoting tumor growth, which have been identified as the diagnostic biomarkers for lung cancer[19], breast cancer[20] and ovarian cancer[21, 22]. The mRNAs found in exosomes can be transferred and translated to functional proteins after uptake by other cells [23]. The RNA content in exosomes varies depending on the cell type and cellular status from their parent cells, for performing cell-to-cell communications[24-29]. The mechanism of how specific RNA sequences are selectively packaged into exosomes is still unknown, but is an intensive area of investigation[8, 30-32].

For investigating cellular communications and behaviors ex vivo, presently, the two-dimensional (2D) cell culture model is widely used as the "golden standard"[33]. This 2D culture system serves as an essential model for investigating tissue physiology and complex biological activity, from cell differentiation to tissue morphogenesis[34]. Many 2D cell culture systems have also been widely employed for studying exosome RNA expression profiles from tumor cells [35], roles in

promoting tumor growth [21], and tumor biomarker discovery [36-38]. Although the 2D culture system provides simple cell attachment and nutrients supply, the flat and hard surface from plastic or glass substrates are unable to represent the in vivo extracellular matrix (ECM) microenvironment in tissue or organs[39]. The monolayer cells under 2D culture condition completely differ from in vivo status where cells grow in three dimensions (3D), in terms of cell morphology, cell-to-cell interactions, growth behavior, and interactions with extracellular matrix [34]. It has been well demonstrated that 2D cell monolayer is unable to represent the physiology of in vivo 3D tissues or organs, due to the substantially different microenvironment (e.g., mechanical and biochemical properties) in tissue architecture[40-45].

Unlike the 2D culture, 3D cell culture is more recognized for mimicking in vivo cellular behavior[45]. Instead of cell-to-cell interaction only by the edge in the 2D culture system, 3D cell culture involves cellular stretch and interactions from all angles, as well as the cell-to-ECM interactions[39]. These interactions aid in promoting cellular signaling transduction and proliferation. For instance, the behaviors of 3D tumor spheroids are more clinically relevant, considering hypoxia in the drug screening research[46]. Skin cells under 3D culture conditions survive better than 2D conditions when exposed to cytotoxic agents [47]. The ECM serves as the scaffold which is critical for the cell adhesion, movement, stretch, proliferation and differentiation, and the prevention of apoptosis [48]. Within the 3D culture environment, we observed that cellular exosome secretion dynamics and molecular contents are altered, compared to the 2D culture derived exosomes. This observation indicates that 3D culture derived exosomal RNA content could reflect in vivo tissue-derived exosomal RNAs. Although a few reports studied the exosome secretion from human plasma and 2D culture system, none of them reported the exosome secretion landscape from 3D culture and their potential for mimicking in vivo tissue system. The exosome biogenesis mechanisms, molecular sorting, vesicle trafficking and releasing are still not well understood so far[12, 30]. Other reports and our observation support that exosome secretion behavior and molecular cargoes are altered by the influence of many factors including parent cell types, physiological and pathological status, and the stimuli from microenvironments[49]. Thus, only exosomes derived from parent cells under biomimetic tissue culture conditions can reflect the in vivo exosomes, which is extremely essential for studying cellular biological function, cell-to-cell communications and signaling transductions accurately. These discoveries could eventually lead to the development of clinically significant exosome biomarkers and therapeutic agents.

In this paper, we observed that 2D culture derived exosomes showed significantly different profiles in terms of secretion dynamics and essential signaling molecular contents (RNAs), compared to the 3D culture derived exosomes. By using the next-generation sequencing of cervical cancer cells and cervical cancer patient plasma-derived exosomal RNA, we observed that 3D culture derived exosomal RNAs may undergo specific sorting process that differ from their parent cells. Most importantly, the 3D culture derived exosomal RNA profile exhibited a much higher similarity (~ 96%) to in vivo circulating exosomes from cervical cancer patient plasma, in comparison with 2D derived exosomal RNA profile. On the other hand, DNA sequencing analysis suggests that culture and growth conditions do not affect the genomic information carried by exosome secretion. By tackling exosomal molecular contents and alterations secreted into interstitial fluids, we can provide an alternative, non-invasive approach for investigating 3D tissue behaviors at the molecular precision. This work could serve as a foundation for building precise model employed in mimicking in vivo tissue system, with exosomes as the molecular vehicle, for investigating tumor biomarkers, drug screening, and understanding tumor progression and metastasis.

Results

Exosome secretion dynamics from the 3D cultured cells significantly differ from the 2D culture system

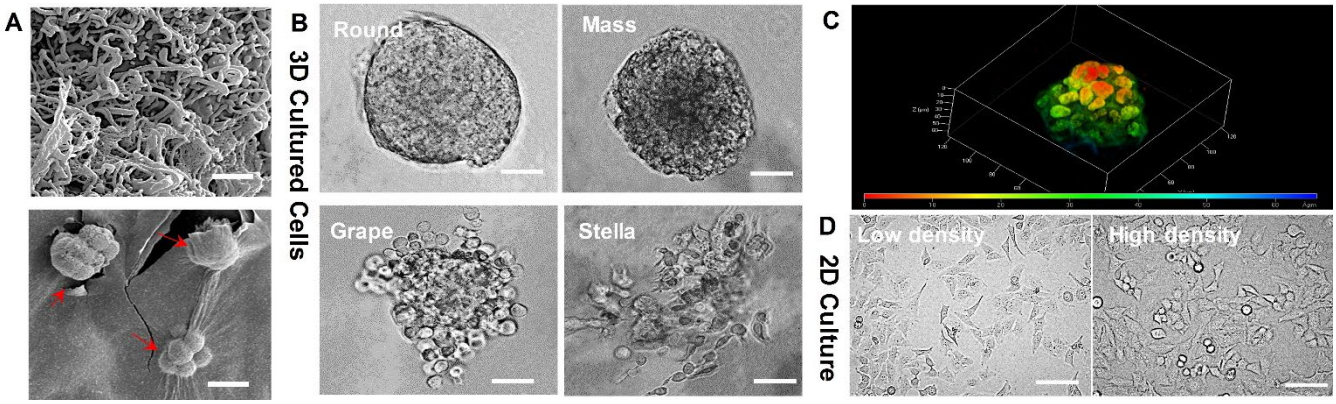

Figure 1. (A) The SEM images showing the morphology of peptide hydrogel as the scaffolds (top, the scale bar is 5μm) for 3D culture of cervical cancer HeLa cells (bottom, the scale bar is 50 μm). (B) The typical 3D cellular morphologies observed

under the bright-field microscopy. The scale bar is 50 μm. (C) The fluorescence confocal microscopic image showing the 3D in-vivo like tumor growth. The 3D confocal image was reconstructed with density distribution and the depth is 60 μm. (D) The 2D cultured cellular morphology in flat spreading with both low density and high-density seeding, which was observed under the bright-field microscopy. The scale bar is 20 μm.

In order to culture in-vivo like 3D cells, we choose to use peptide hydrogel as the scaffolding material which has high biocompatibility and self-healing property for transforming between liquid and gelation[50-52]. This peptide hydrogel is stable in neutral pH and remains as gel formation in a wide range of temperatures from 2° C to 80° C[53, 54]. We examined the peptide hydrogel scaffolding structures in Figure 1 A to evaluate the 3D ECM microenvironment, which shows the dense mesh network with pore size nearly around 500 nm. The flexible mechanical tensile of peptide gel allows cells to proliferate and expand as a 3D spheroid. Due to the high biocompatibility, the big 3D spheroid still can attach well with the scaffolding support. We observed four classic morphologies presented in the 3D cultured spheroids with peptide hydrogel scaffolds: round, mass, grape, and stellate, as shown in Figure 1B. Confocal fluorescence image was further used to confirm the round tumor morphology in Figure 1C, which exhibits the typical in vivo tumor-like tissue architecture. The cervical cancer HeLa cells formed the round spheroids after 4-5 days culture which are the most typical tumor morphology dominated in our 3D culture system. The grape and stellate shapes were observed occasionally. In strong contrast, 2D cultured HeLa cells are in the flat spreading and attached to the bottom of the culture plate, which is substantially lacking cell-to-cell contact, as shown in Figure 1D. Even though in the high-density culture condition, the cell contacts in 2D are only through the cell edges with much loose communication.

We further examined the exosome secretion rate by using nanoparticle tracking analysis (NTA) to monitor the exosomes derived from both 2D culture and 3D culture systems under different culture durations. For 3D cells, the culture can reach 90% confluence after 11 days which is much slower than the 2D culture system. So we followed the comparable cellular growth status to collect exosomes. For 2D cultured cells, we harvest exosomes from media in 6h, 12h, 24h, 36h, and 48h intervals, while 3D culture derived exosomes are harvested at day 5, 7, 9, 11, and 13, individually. The exosome secretion rate from the 3D cultured cells is more active when cells approach the confluence, which is reflected by three times more exosomes secreted after day 9. In contrast, 2D cultured cells reduce the exosomes secretion and undergo a declining trend, which may attribute to the reduced cell-to-cell contact and communication. The harvested exosomes showed typical round, cup-shape via SEM imaging with an average size around 100 nm in both 2D and 3D culture conditions (Figure 2 B and D).

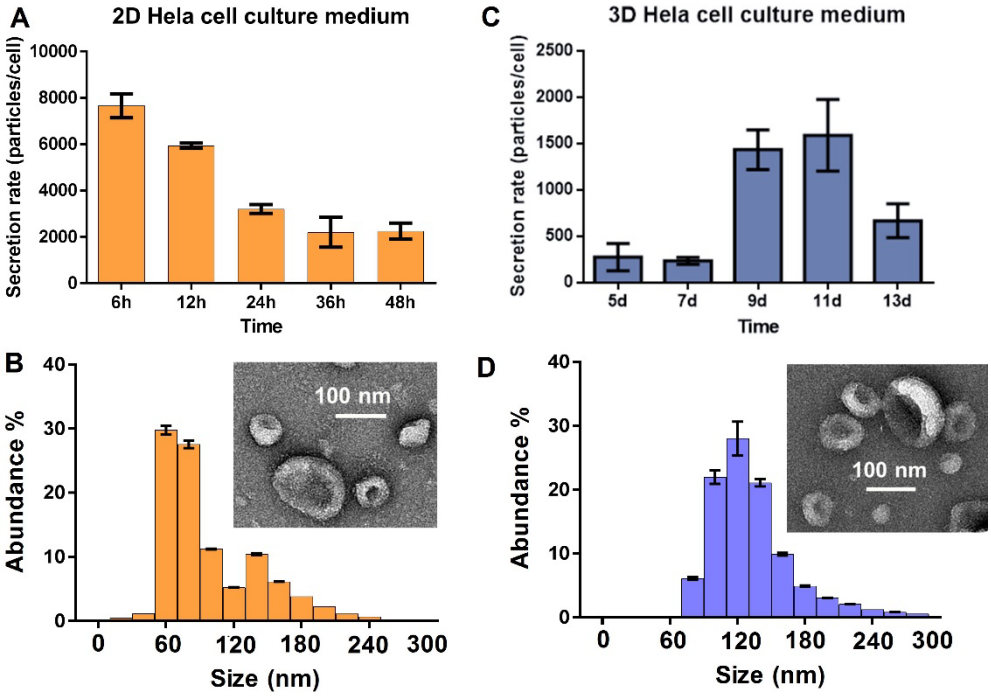

Figure 2. The nanoparticle tracking analysis (NTA) of exosome secretion rate between 2D culture (A) and 3D culture (B) systems. The harvested exosomes from 2D (B) and 3D (D) culture conditions showed typical round, cup-shape around 100 nm size via SEM imaging (Insert).

The 3D cell culture derived exosomal RNA profile shows a significantly high similarity to in vivo exosomal RNA profile
In order to investigate the exosomal RNA profiles which are altered under different culture conditions with their parent cells, we prepared multiple exosomal RNA extracts as analyzed in Figure 3 by Agilent Bioanalyzer, including exosomal RNAs derived from 2D culture, 3D culture, and cervical cancer patient plasma, compared with parent cell RNAs in 2D and 3D culture conditions. In contrast to their parent HeLa cell-derived RNAs which are mainly in the long size range (2000-4000 nucleotides), exosomes carry more small RNAs around the range below 200 nucleotides. Several studies have shown that exosomes carry small coding and noncoding RNAs used by their parent cells as an intercellular network of communication. Thus, there is a selective packaging process for loading RNAs into exosomes shedding into extracellular microenvironment for modifying the phenotype of the recipient cells, although the mechanisms underlying are still largely unknown[31]. Parent cells take up solutes, nutrients, and ligands from extracellular environment via the multiple endocytic pathways and traffic via early endosomes[30]. From endosome maturation into late endosomes, inward budding from the limiting membrane of the endosome leads to the formation of multi-vesicular bodies (MVBs) containing intraluminal vesicles (ILVs), and then fuse with the plasma membrane to release their ILVs into the extracellular space as exosomes[30]. During MVB formation, cytosolic RNAs are taken up into ILVs undergoing inward budding with a selective lipid-mediated loading of RNA into exosomes[32]. A few RNA-binding proteins have been found capable to selectively bind RNA molecules with specific motifs and induce their export into exosomes, such as hnRNPA2B1[30, 55]. Therefore, we can observe a significant amount of small regulatory RNAs enriched in exosomes, but not significant in their parent HeLa cells, regardless of 2D or 3D culture conditions. Because the HeLa cell line is the established cell line from the cervical cancer patient, we further compared the exosomal RNA extract from the cervical cancer patient plasma which also are mainly small coding and non-coding RNAs.

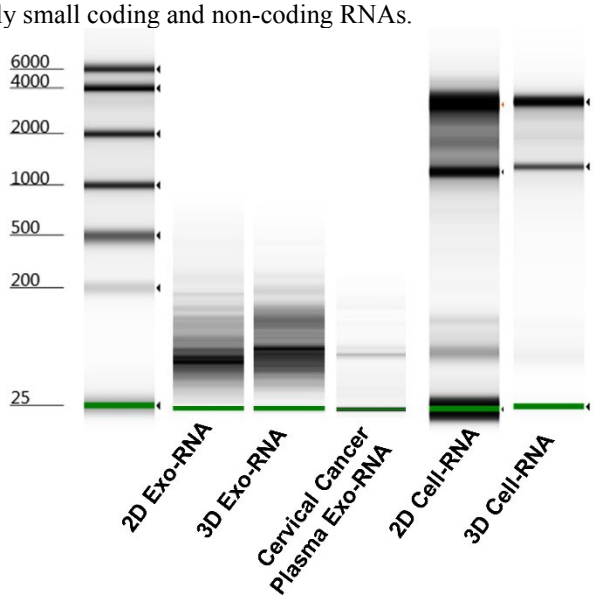

Figure 3. Bioanalyzer analysis of exosomal RNAs derived from 2D culture, 3D culture, and cervical cancer patient plasma, compared with parent cell RNAs in 2D and 3D culture conditions.

For further understanding the landscape of exosomal RNA compositions under different culture conditions of their parent cells, and providing an accurate profile of the different coding and non-coding RNA species found per culture compartment, we did small RNAs library preparation (< 200 nt) and used the next generation sequencing to characterize exosome derived RNAs and parent cell RNAs in depth. The resulting reads were aligned to the RefSeq transcriptome annotation (version hg38, downloaded from the UCSC genome browser), the GENCODE (version 28 for hg38), tRNA annotation tracks (version hg38, downloaded from the UCSC genome browser), and the miRNA annotations tracks (version hg38, downloaded from sRNAnalyzer database), using BWA[16]. Only the uniquely aligned reads were considered for downstream analysis. A significant portion (>90%)of the reads were mapped as mRNAs while a much smaller fraction of the reads were mapped as other non-coding RNAs , as shown in Figure 4. It is worth mentioning that exosomal miRNA contents from cervical cancer patient plasma are clearly higher than the healthy individual (3:1).

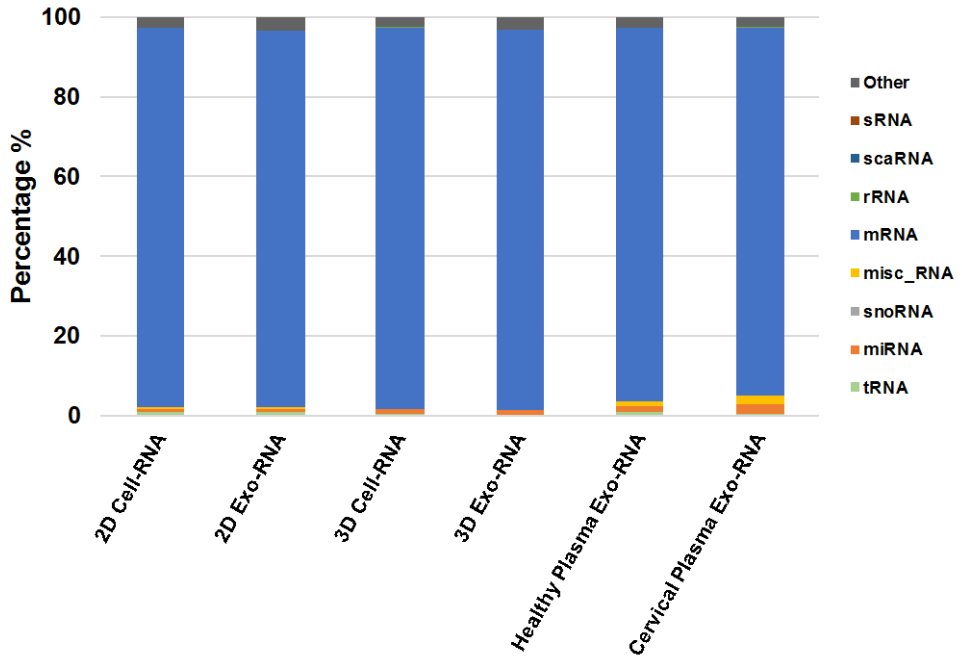

Figure 4. Graph depicting the percentage of reads mapped to transcriptomic regions. The majority of the sequences (>90%) belonged to the protein coding region (mRNA's) of the transcriptome. The remaining fraction was mapping to the non-coding regions of the transcriptome. Mapping sequences from 2D and 3D cell culture, exosomal 2D and 3D cultures, exosomal cervical cancer patient plasma and exosomal healthy patient plasma cultures were used for analysis.

The next-generation RNA-Seq profiling of exosomal miRNAs from biopsy specimens is a relatively underexplored frontier. To compare the exosomal miRNA content derived from various samples, the top 100 miRNAs with the highest average abundances in all samples were selected, and their abundance profiles were subsequently clustered (see Figure 5). As anticipated, replicates (2D-cell samples and 3D-cell samples) were clustered together. More importantly, the 3D cell-derived exosome sample was clustered together with two in vivo cervical cancer patient plasma samples. It shows that 3D cell culture is necessary for reproducing the exosomal miRNA content sorted by in vivo cells, and establishing an accurate disease model. On the other hand, the 2D-derived samples were clustered away from the in vivo samples, indicating that 2D cell culture was unable to represent in vivo biological status. It is interesting that multiple miRNAs were identified from 3D cell-derived exosomes as well as the cervical cancer patient plasma-derived exosomes, but not 2D culture derived exosomes, such as hsa-miRNA- 2277, hsa-miRNA-3691, hsa-miRNA-4488, hsa-miRNA- 548ao, hsa-miRNA-6871, hsa-miRNA-93, hsa-miRNA-4763, hsa-miRNA-6751, and hsa-miRNA- 4633-5p, which are highly associated with control of stability and translation of mRNA [56] [57] [58].

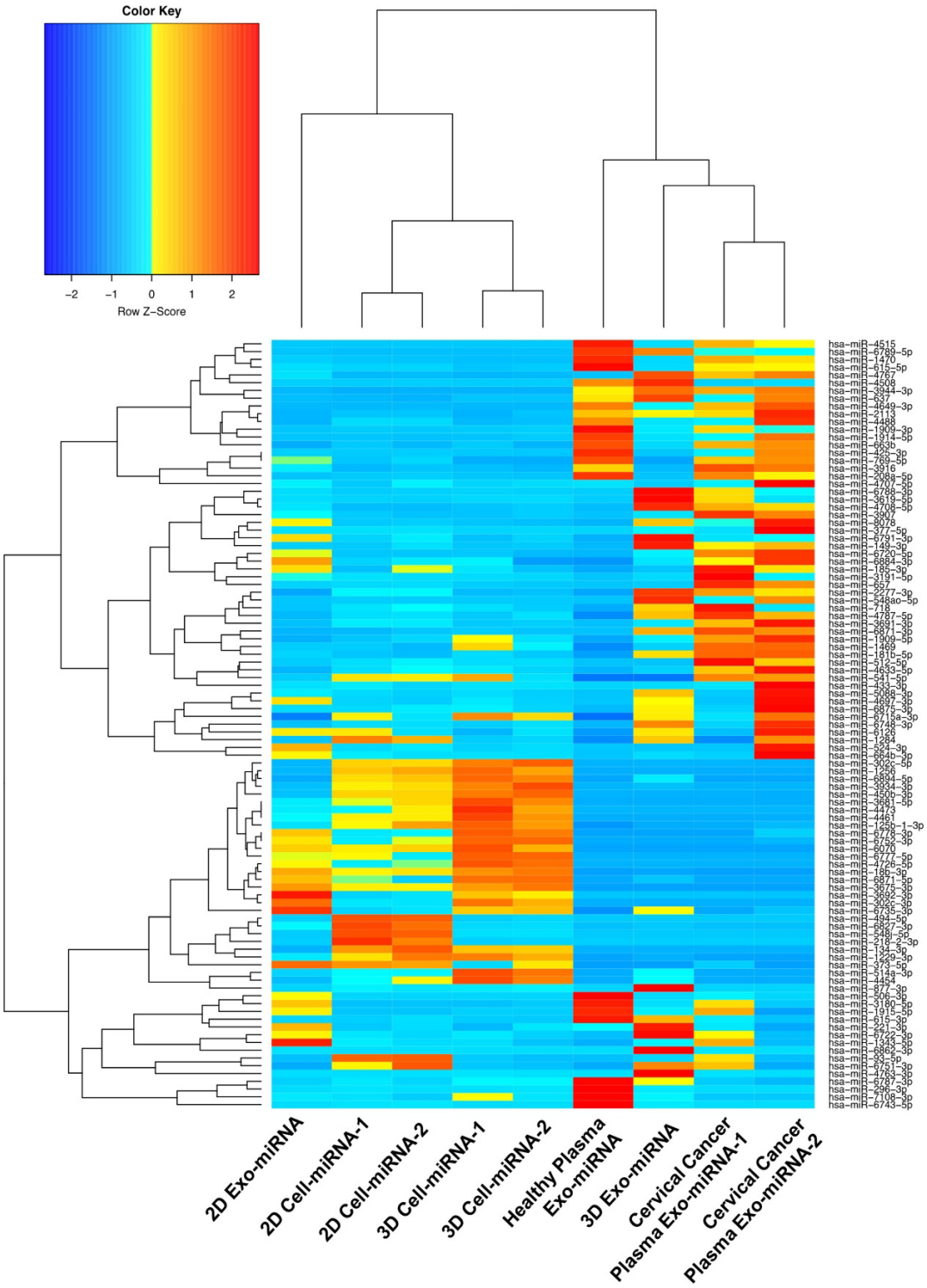

Figure 5. Heatmap with dendogramn depicting top 100 highly expressed miRNAs in 2D Cell, 3D Cell, and their derived exosomal miRNAs in relation to cervical cancer patient plasma exosomal miRNAs and healthy plasma exosome miRNAs. Red color indicates a higher expression z-score. Hierarchical clustering was performed, using the Spearman correlation method. 3D exosomal miRNA profile and Cervical cancer patient plasma exosomal miRNA profile have been clustered together due to higher similarities in their transcript expressions.

We further performed region-based annotation on the exosomal RNA reads, using ANNOVAR [17]. Most of the reads (~90%) belonged to the Intronic, Intergenic, Upstream and UTR5 regions, and their distributions are shown in Figure 6. The remaining reads (10-12%) were mapped to other whole genomic regions (Exonic, Splicing, UTR3, Downstream). The results again showed significant similarity between the 3D cell-derived exosomal RNAs and in vivo cervical cancer patient plasma-derived exosomal RNAs, reconfirming the advantage of our 3D cell culturing method.

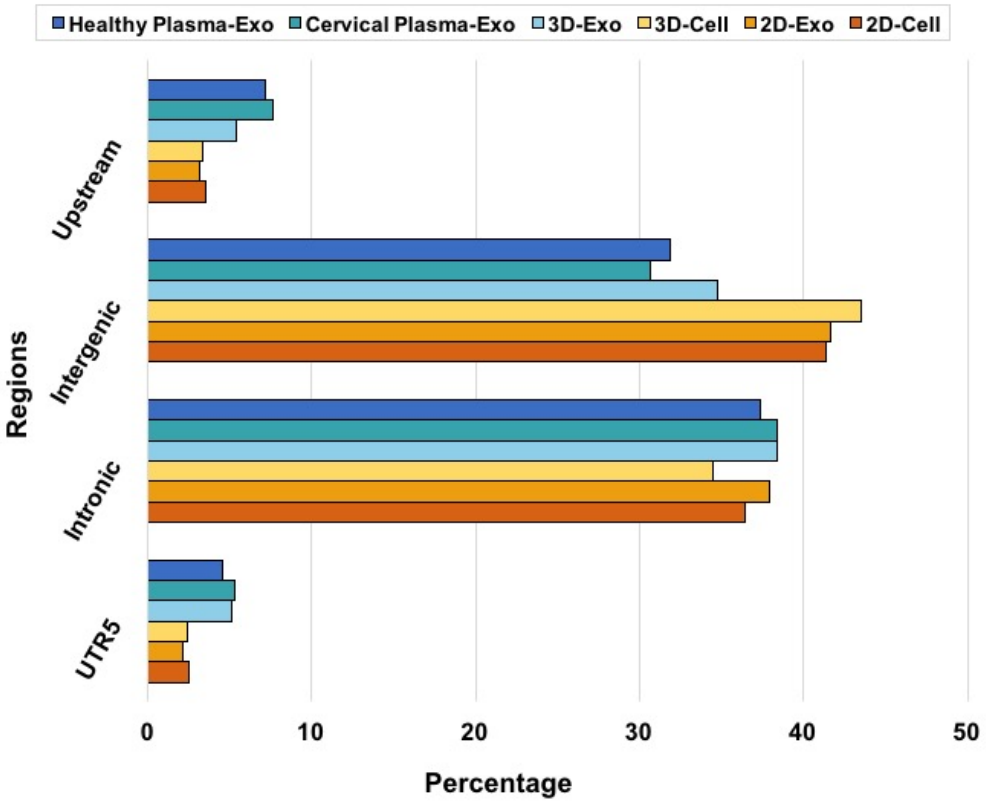

Figure 6. Bar graph depicting the percentage of reads mapped to whole genome regions. The majority of the sequences belong to Intronic, Intergenic, Upstream and UTR5 regions of the whole genome nucleotide sequences from 2D and 3D cell cultures. Comparisons were made with nucleotide sequences derived from cervical and healthy patient plasma exosomes.

The 3D cell culture derived exosomal DNA profiling

We also performed the extraction of exosome DNA for analyzing DNA sequences between different cultures of their parent cell. The quality of extracted exosomal DNA was assessed by Agilent ChipStation shown in Figure 7 A. Most of the DNA fragments were genomic DNAs and smaller than 1000 nucleotides. Highly correlated DNA fragment length distributions of the 2D and 3D culturing methods were observed. The reads were mapped to the reference genomes obtained from RefSeq (version hg38), using BWA aligner. The Spearman correlation of the protein-coding gene abundances between samples were calculated and shown in Figure 7B. The results reaffirm that all samples have high abundance correlation, showing that the exosomal DNA content is more stable than the RNA content, and appears recalcitrant to various culturing methods.

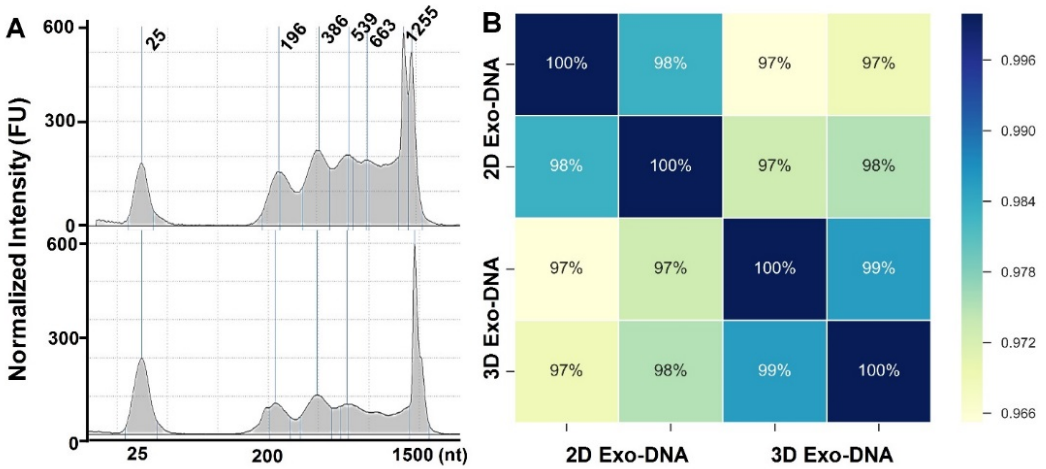

Figure 7. (A) Quality analysis of extracted exosomal DNAs derived from 2D culture (top) and 3D culture (bottom). (B) The correlation matrix of the DNAseq reads from two samples each of 2D and 3D exosome samples using the Spearman correlation coefficient. The two samples belonging to the same category (2D Exo-DNA or 3D Exo-DNA) are highly similar to each other.

For the DNA reads that were not mapped as protein-coding genes, we further predict their mapped regions (peaks) using HOMER. Similar to the protein-coding abundance profile, the predicted peaks also show high abundance correlation between the 2D and 3D samples. Based on the above observations, the culture and growth conditions do not affect the genomic information carried by exosome secretion. The recent report also discovered that serum-derived exosomal dsDNA was highly consistent with the paired tumor genome, which is essential evidence that exosomal DNA can be used as a genetic marker for cancer diagnosis via screening gene mutations[59].

Discussion

Exosomes are important non-contact cellular communication pathways for horizontally transferring genetic information. Intensive studies have been devoted to this research field in recent five years showing that exosomal miRNAs play an important role in disease progression, angiogenesis, and cancer metastasis[60, 61]. The sequencing approaches for studying exosomal RNAs and DNAs have been a spotlight in recent two years. However, using the right sample sources and cellular model systems are very critical. The cellular secretion of exosomes is a dynamic process and reflects the microenvironmental changes or parent cell stress. Our study in this paper also demonstrated that culture conditions could induce the exosomal RNA change, especially for miRNAs which have been well recognized as the crucial cancer diagnostic biomarkers. Exosomes carry miRNAs which can be taken up by neighboring or distant cells for modulating recipient cells. Our observation[30, 31] and other reports both observed that miRNA profiles of exosomes differ from those of the parent cells, indicating that an active sorting mechanism of exosomal miRNAs may present.

We also observed that exosome miRNAs are sensitive to their parent cell culture conditions. Our study compared the exosomal RNAs derived from 2D culture and 3D culture of cervical cancer cells, in relation to human plasma exosomal RNAs from cervical cancer patients. This result is an evidence showing that nearly ~ 96% similarity exists between 3D culture derived exosomal miRNAs and cervical cancer patient plasma-derived exosomal miRNAs. On the contrary, 2D culture derived exosomal miRNAs does not correlate as highly with human plasma exosomal RNA profile (~80%). For accurately understanding the real cellular communication in a biological system, the in vivo and real-time collected exosomes can better reflect the cellular –level communications. However, obtaining in vivo samples are always challenging due to limited access and regulatory issues. Therefore, building the ex-vivo cellular model is absolutely needed. The 3D culture protocols established in our lab using peptide hydrogel could produce cells with the secretion of in-vivo like exosomes. This discovery also can lead to a viable and non-destructive approach for studying tissues and organs via collecting exosomes from interstitial fluids or culture medium. By analysis of exosomal DNA sequencing data, we observed that culture or growth conditions do not affect the genomic information carried by exosome secretion, which is supported by recent reports which used exosomal DNA as their parent tumor surrogate for cancer diagnosis[62, 63].

Methods

2D and 3D cell culture: Hela-cell (ATCC® CCL-2™) were maintained by MEM complete medium (L-glucose MEM medium, Gibco, 11095072) with 10% (v/v) exosome-depleted fetal bovine serum (Gibco, A2720801) at 37 ℃ with 5% CO_2. To subculture the cell, the cells were digested by 0.25% trypsin (Gibco, 25200-056) and resuspend by fresh MEM medium when the confluence reached to 90%. The 1:5 ratio of resuspended cells were taken to a new flask and maintained the culture until the next subculture. The 3D culture process was carried out by using the commercial PGmatrix DMEM Kit (Pep GEL LLC, PGD-006) per vendor's protocol. Hela-cells were seeded into the peptide hydrogel with density ~ 8×10^4 which was measured by an automated cell counter (Millipore Corporation, PHCC3000). The 3D culture was maintained using a 24-well cell culture plate with ~ 390 µL cell suspension, 10 µL PGworks solution, and 100 µL PGmatrix solution. The mixture was mixed by pipetting up and down carefully without introducing any bubbles. The well plate was placed into the 37 °C incubators for 1 h. After gelation, 1000 µL warmed fresh MEM complete medium was added to the top of the gel without disturbing. The medium exchange was performed every other day for supplying fresh nutrition and preventing drying out of hydrogel due to long-term culture. The ZOE™ Fluorescent Cell Imager (Bio-Rad Laboratories) was used to observe growth behavior with multiple time intervals.

Exosome isolation and NTA analysis: 2D cultured medium was collected at 6, 12, 24, 36, 48, and 60 hours post subculture. The 3D cultured medium was collected at 1, 3, 5, 7, 9, 11, 13, 15 days post subculture. To remove the cell debris, the medium was centrifuged at 10,000g for 20 min within 4 °C, and then discard the supernatant carefully without disturbing the pellet at the bottom of the tube. The Nanoparticle Tracking Analysis (NTA) was performed to measure the particle concentration and size distribution using NanoSight LM10 (Malvern Instruments). For recovering 3D spheroids, the scaffolding hydrogels were broken mechanically by pipetting up and down, and then transferred into a 15 mL tube for centrifuging at 600 g for 10 min at room temperature for collecting cell pellet. ~0.5 mL 0.25% trypsin (Gibco, 25200-056) was added into the pellet, resuspended gently, and then incubated at 37 °C for 5 min. The trypsin digestion was stopped by adding 0.5 mL MEM complete medium.

Exosomal RNA extraction: The culture media from the 2D and 3D cultures were harvested when the confluence reached ~90%. Based on the log phase of growth of 3D cells, exosomes were harvested after 11 days of a subculture which is comparable to the confluence as the 2D culture. The medium was processed using a centrifuge at 1500g for 30 min to remove the remaining cell debris and then apply a 0.22 µm filter to collect exosomes. The exosomal RNAs were extracted using the exoRNeasy Serum/Plasma Starter Kit (Qiagen, 77023) following the vendor's instruction. The Agilent Bioanalyzer 2100 Small RNA Chip (Agilent Technologies) was used to determine the quality of the exosomal RNA.

The frozen human plasma samples were obtained from the University of Kansas Cancer Center Biorepository. ~3 mL human plasma was centrifuged at 3000g for 15 min at 4 °C, and then transfer the supernatant to a centrifuge tube without disturbing the pellet for spinning at 10,000g with 20 min in 4 °C. Then the supernatant was carefully discard without disturbing the pellet at the bottom of the tube. The equal volume of buffer XBP was added to the tube and then apply a 0.22 µm filter to collect exosomes. Exosomal RNA was extracted by using the exoRNeasy Serum/Plasma Starter Kit (Qiagen, 77023).

Exosome DNA extraction: The exosomal DNAs were extracted by the combination of the QIAamp DNA Mini Kit (Qiagen, 51304) and the exoRNeasy Serum/Plasma Starter Kit (Qiagen, 77023) following the vendor's instruction. ~4 mL cell culture medium were used to isolate exosomes. The exoEasy spin column was used for spinning at 500 g for 1min. The flow-through medium was discarded and spin again for 1 min at 3,200 g. ~10 mL XWP buffer was added to the column and spin for 10 min at 3,200 g to wash the trapped exosomes in the membrane of spin column. The QIAamp DNA Mini Kit was used to extract the exosomal DNA. ~ 400 µL PBS buffer, 40 µL QIAGEN Protease, and 4 µL RNase (Qiagen, 19101) were mixed into one 1.5 microcentrifuge tube and transferred into the center of the column membrane for wetting the membrane. ~400 µL AL buffer was added to the membrane slowly and mixed by pipette up and down without touching the membrane. The resulted column was incubated for 10 min at 56 °C, and then spin for 10 min at 3,200 g to collect the flow-through lysate into a new 1.5 mL microcentrifuge tube. ~ 400 µL ethanol was added to the lysate and mixed for 15 s. The QIAmp Mini spin column was used for spinning at 6,000g for 1 minute. Then the column membrane was washed with 500 µL AW1 buffer and AW2 buffer separately provided in the kit. The DNA concentration was measured by Qubit® 3.0 Fluorometer (Life Technologies, Q33216).

Sequencing and data analysis: The RNA library was prepared by using the commercial library preparation kit NEXTflex small RNA sequencing kit (Bioo Scientific, NOVA-5132-05) following the recommended protocol by the manufactures. The amplified libraries were examined by the TapeStation gel (Angilent 2200). The DNA peaks with 150 bp were purified by the gel size selection approach and eluted in ~ 8 µL elution buffer. The sequencing was performed by the KU Genomic Core using the Illumina HiSeq 2500 System. Raw reads were trimmed to remove the 3' adaptor sequences. The sequences were filtered by removing sequences with lengths <16 nt. The filtered sequences were mapped onto the RefSeq transcriptome annotation (version hg38, downloaded from the UCSC genome browser), GENCODE (version 28 for hg38), tRNA annotation tracks (version hg38, downloaded from the UCSC genome browser), and the miRNA annotations tracks (version hg38, downloaded from sRNAnalyzer database). The RefSeq whole genome annotation was used to perform region-based annotation. Mapping was performed uing BWA Aligner. Only a single optimal hit was retrieved, by setting the parameter R=1, during alignment. Differences in seed length were disallowed (set k=0). All other parameters were set to default. A comparison between the percentage of reads mapped using single hit parameter (R=1) and the default parameter, which allows multiple hits (R=30) is shown in Table 1. It was observed that the mapping percentages were higher when multiple hits were allowed, as opposed to a single best hit. However, since the sample sequences used were very short (<100bps), the sub-optimal hits obtained were most likely to be false positive alignments, thereby making them unsuitable for our analysis purposes.

Table 1. BWA mapping percentages of filtered nucleotide sequences with parameters –R 1 (only single hit) and –R 30 (default parameter- allows multiple hits), for whole genomic and transcriptomic regions.

		Whole Genome		Transcriptome	
Type	**Number of sequences**	**R=1**	**R=30**	**R=1**	**R=30**
2D-1	4582381	37.33	45.91	24.56	33.08
2D-2	3648233	33.60	42.19	21.98	29.61
2D-Exo	11446338	23.58	31.03	12.55	18.70
3D-1	4597454	24.76	31.26	19.57	22.80
3D-2	3857048	23.74	30.41	18.66	21.78
3D-Exo	1265596	52.50	60.82	34.04	47.44
Plasma-Healthy Exo	7719847	7.29	10.39	4.88	6.77
Plasma-Cervical-1 Exo	6111748	9.40	12.90	6.28	8.63
Plasma-Cervical-2 Exo	4718015	9.69	11.80	6.75	8.96

References

1. Deatherage BL, Cookson BT: **Membrane vesicle release in bacteria, eukaryotes, and archaea: a conserved yet underappreciated aspect of microbial life**. *Infection and immunity* 2012, **80**(6):1948-1957.
2. Wolf P: **The nature and signifcance of platelet products in human plasma**. *Br J Haematol* 1967, **13**:9.
3. Anderson HC: **Vesicles associated with calcifcation in the matrix of epiphyseal cartilage**. *J Cell Biol* 1969, **41**:13.
4. Kalluri R: **The biology and function of exosomes in cancer**. *J Clin Invest* 2016, **126**(4):1208-1215.
5. Gyorgy B, Szabo TG, Pasztoi M, Pal Z, Misjak P, Aradi B, Laszlo V, Pallinger E, Pap E, Kittel A *et al*: **Membrane vesicles, current state-of-the-art: emerging role of extracellular vesicles**. *Cell Mol Life Sci* 2011, **68**(16):2667-2688.
6. van Niel G, D'Angelo G, Raposo G: **Shedding light on the cell biology of extracellular vesicles**. *Nat Rev Mol Cell Biol* 2018, **19**(4):213-228.
7. Hessvik NP, Llorente A: **Current knowledge on exosome biogenesis and release**. *Cell Mol Life Sci* 2018, **75**(2):193-208.
8. Shen B, Fang Y, Wu N, Gould SJ: **Biogenesis of the posterior pole is mediated by the exosome/microvesicle protein-sorting pathway**. *J Biol Chem* 2011, **286**(51):44162-44176.
9. Pant S, Hilton H, Burczynski ME: **The multifaceted exosome: biogenesis, role in normal and aberrant cellular function, and frontiers for pharmacological and biomarker opportunities**. *Biochem Pharmacol* 2012, **83**(11):1484-1494.

10. Fares J, Kashyap R, Zimmermann P: **Syntenin: Key player in cancer exosome biogenesis and uptake?** *Cell Adh Migr* 2017, **11**(2):124-126.
11. Raposo G, Stoorvogel W: **Extracellular vesicles: Exosomes, microvesicles, and friends**. *The Journal of Cell Biology* 2013, **200**(4):373-383.
12. Shao H, Im H, Castro CM, Breakefield X, Weissleder R, Lee H: **New Technologies for Analysis of Extracellular Vesicles**. *Chem Rev* 2018, **118**(4):1917-1950.
13. Kruger S, Abd Elmageed ZY, Hawke DH, Worner PM, Jansen DA, Abdel-Mageed AB, Alt EU, Izadpanah R: **Molecular characterization of exosome-like vesicles from breast cancer cells**. *BMC Cancer* 2014, **14**:44.
14. Saeedi Borujeni MJ, Esfandiary E, Taheripak G, Codoner-Franch P, Alonso-Iglesias E, Mirzaei H: **Molecular aspects of diabetes mellitus: Resistin, microRNA, and exosome**. *J Cell Biochem* 2018, **119**(2):1257-1272.
15. Wan Z, Gao X, Dong Y, Zhao Y, Chen X, Yang G, Liu L: **Exosome-mediated cell-cell communication in tumor progression**. *Am J Cancer Res* 2018, **8**(9):1661-1673.
16. Samuelson I, Vidal-Puig AJ: **Fed-EXosome: extracellular vesicles and cell-cell communication in metabolic regulation**. *Essays Biochem* 2018, **62**(2):165-175.
17. Maia J, Caja S, Strano Moraes MC, Couto N, Costa-Silva B: **Exosome-Based Cell-Cell Communication in the Tumor Microenvironment**. *Front Cell Dev Biol* 2018, **6**:18.
18. Zhang W, Peng P, Shen K: **Role of Exosome Shuttle RNA in Cell-to-Cell Communication**. *Zhongguo Yi Xue Ke Xue Yuan Xue Bao* 2016, **38**(4):480-483.
19. Zhang D, Lee H, Wang X, Rai A, Groot M, Jin Y: **Exosome-Mediated Small RNA Delivery: A Novel Therapeutic Approach for Inflammatory Lung Responses**. *Mol Ther* 2018, **26**(9):2119-2130.
20. Jia Y, Chen Y, Wang Q, Jayasinghe U, Luo X, Wei Q, Wang J, Xiong H, Chen C, Xu B *et al*: **Exosome: emerging biomarker in breast cancer**. *Oncotarget* 2017, **8**(25):41717-41733.
21. Skog J, Wurdinger T, van Rijn S, Meijer D, Gainche L, Sena-Esteves M, Curry WT, Carter RS, Krichevsky AM, Breakefield XO: **Glioblastoma microvesicles transport RNA and protein that promote tumor growth and provide diagnostic biomarkers**. *Nature cell biology* 2008, **10**(12):1470-1476.
22. Shen J, Zhu X, Fei J, Shi P, Yu S, Zhou J: **Advances of exosome in the development of ovarian cancer and its diagnostic and therapeutic prospect**. *Onco Targets Ther* 2018, **11**:2831-2841.
23. Valadi H, Ekstrom K, Bossios A, Sjostrand M, Lee JJ, Lotvall JO: **Exosome-mediated transfer of mRNAs and microRNAs is a novel mechanism of genetic exchange between cells**. *Nat Cell Biol* 2007, **9**(6):654-659.
24. Wang J, Barr MM: **Cell-cell communication via ciliary extracellular vesicles: clues from model systems**. *Essays Biochem* 2018, **62**(2):205-213.
25. Mathieu M, Martin-Jaular L, Lavieu G, Thery C: **Specificities of secretion and uptake of exosomes and other extracellular vesicles for cell-to-cell communication**. *Nat Cell Biol* 2019, **21**(1):9-17.
26. Hwang I: **Cell-cell communication via extracellular membrane vesicles and its role in the immune response**. *Mol Cells* 2013, **36**(2):105-111.
27. Tetta C, Ghigo E, Silengo L, Deregibus MC, Camussi G: **Extracellular vesicles as an emerging mechanism of cell-to-cell communication**. *Endocrine* 2013, **44**(1):11-19.
28. Turturici G, Tinnirello R, Sconzo G, Geraci F: **Extracellular membrane vesicles as a mechanism of cell-to-cell communication: advantages and disadvantages**. *Am J Physiol Cell Physiol* 2014, **306**(7):C621-633.
29. Wendler F, Stamp GW, Giamas G: **Tumor-Stromal Cell Communication: Small Vesicles Signal Big Changes**. *Trends Cancer* 2016, **2**(7):326-329.
30. Zhang J, Li S, Li L, Li M, Guo C, Yao J, Mi S: **Exosome and exosomal microRNA: trafficking, sorting, and function**. *Genomics Proteomics Bioinformatics* 2015, **13**(1):17-24.
31. Villarroya-Beltri C, Baixauli F, Gutierrez-Vazquez C, Sanchez-Madrid F, Mittelbrunn M: **Sorting it out: regulation of exosome loading**. *Semin Cancer Biol* 2014, **28**:3-13.

32. Subra C, Laulagnier K, Perret B, Record M: **Exosome lipidomics unravels lipid sorting at the level of multivesicular bodies**. *Biochimie* 2007, **89**(2):205-212.
33. Lampe KJ, Mooney RG, Bjugstad KB, Mahoney MJ: **Effect of macromer weight percent on neural cell growth in 2D and 3D nondegradable PEG hydrogel culture**. *J Biomed Mater Res A* 2010, **94**(4):1162-1171.
34. Tibbitt MW, Anseth KS: **Hydrogels as Extracellular Matrix Mimics for 3D Cell Culture**. *Biotechnology and bioengineering* 2009, **103**(4):655-663.
35. Honegger A, Schilling D, Bastian S, Sponagel J, Kuryshev V, Sültmann H, Scheffner M, Hoppe-Seyler K, Hoppe-Seyler F: **Dependence of Intracellular and Exosomal microRNAs on Viral E6/E7 Oncogene Expression in HPV-positive Tumor Cells**. *PLoS Pathogens* 2015, **11**(3):e1004712.
36. Kahlert C, Melo SA, Protopopov A, Tang J, Seth S, Koch M, Zhang J, Weitz J, Chin L, Futreal A *et al*: **Identification of Double-stranded Genomic DNA Spanning All Chromosomes with Mutated KRAS and p53 DNA in the Serum Exosomes of Patients with Pancreatic Cancer**. *The Journal of Biological Chemistry* 2014, **289**(7):3869-3875.
37. Taylor DD, Gercel-Taylor C: **MicroRNA signatures of tumor-derived exosomes as diagnostic biomarkers of ovarian cancer**. *Gynecologic oncology* 2008, **110**(1):13-21.
38. Zhao Z, Yang Y, Zeng Y, He M: **A Microfluidic ExoSearch Chip for Multiplexed Exosome Detection Towards Blood-based Ovarian Cancer Diagnosis()**. *Lab on a chip* 2016, **16**(3):489-496.
39. Pampaloni F, Reynaud EG, Stelzer EHK: **The third dimension bridges the gap between cell culture and live tissue**. *Nature Reviews Molecular Cell Biology* 2007, **8**:839.
40. Li Y, Kilian KA: **Bridging the Gap: From 2D Cell Culture to 3D Microengineered Extracellular Matrices**. *Adv Healthc Mater* 2015, **4**(18):2780-2796.
41. Marino S, Bishop RT, de Ridder D, Delgado-Calle J, Reagan MR: **2D and 3D In Vitro Co-Culture for Cancer and Bone Cell Interaction Studies**. *Methods Mol Biol* 2019, **1914**:71-98.
42. Duval K, Grover H, Han LH, Mou Y, Pegoraro AF, Fredberg J, Chen Z: **Modeling Physiological Events in 2D vs. 3D Cell Culture**. *Physiology (Bethesda)* 2017, **32**(4):266-277.
43. Lou E, O'Hare P, Subramanian S, Steer CJ: **Lost in translation: applying 2D intercellular communication via tunneling nanotubes in cell culture to physiologically relevant 3D microenvironments**. *FEBS J* 2017, **284**(5):699-707.
44. Barros AS, Costa EC, Nunes AS, de Melo-Diogo D, Correia IJ: **Comparative study of the therapeutic effect of Doxorubicin and Resveratrol combination on 2D and 3D (spheroids) cell culture models**. *Int J Pharm* 2018, **551**(1-2):76-83.
45. Souza AG, Silva IBB, Campos-Fernandez E, Barcelos LS, Souza JB, Marangoni K, Goulart LR, Alonso-Goulart V: **Comparative Assay of 2D and 3D Cell Culture Models: Proliferation, Gene Expression and Anticancer Drug Response**. *Curr Pharm Des* 2018, **24**(15):1689-1694.
46. Breslin S, O'Driscoll L: **Three-dimensional cell culture: the missing link in drug discovery**. *Drug Discovery Today* 2013, **18**(5):240-249.
47. Sun T, Jackson S, Haycock JW, MacNeil S: **Culture of skin cells in 3D rather than 2D improves their ability to survive exposure to cytotoxic agents**. *Journal of Biotechnology* 2006, **122**(3):372-381.
48. Kleinman HK, Philp D, Hoffman MP: **Role of the extracellular matrix in morphogenesis**. *Current Opinion in Biotechnology* 2003, **14**(5):526-532.
49. Minciacchi VR, Freeman MR, Di Vizio D: **Extracellular Vesicles in Cancer: Exosomes, Microvesicles and the Emerging Role of Large Oncosomes**. *Seminars in cell & developmental biology* 2015, **40**:41-51.
50. Chatterjee K, Young MF, Simon CG, Jr.: **Fabricating gradient hydrogel scaffolds for 3D cell culture**. *Comb Chem High Throughput Screen* 2011, **14**(4):227-236.
51. Benson K, Galla HJ, Kehr NS: **Cell adhesion behavior in 3D hydrogel scaffolds functionalized with D- or L-aminoacids**. *Macromol Biosci* 2014, **14**(6):793-798.

52. Gu J, Zhao Y, Guan Y, Zhang Y: **Effect of particle size in a colloidal hydrogel scaffold for 3D cell culture**. *Colloids Surf B Biointerfaces* 2015, **136**:1139-1147.
53. Wang X, Wang J, Guo L, Wang X, Chen H, Wang X, Liu J, Tredget EE, Wu Y: **Self-assembling peptide hydrogel scaffolds support stem cell-based hair follicle regeneration**. *Nanomedicine* 2016, **12**(7):2115-2125.
54. Reis LA, Chiu LL, Liang Y, Hyunh K, Momen A, Radisic M: **A peptide-modified chitosan-collagen hydrogel for cardiac cell culture and delivery**. *Acta Biomater* 2012, **8**(3):1022-1036.
55. Tian T, Zhu YL, Hu FH, Wang YY, Huang NP, Xiao ZD: **Dynamics of exosome internalization and trafficking**. *J Cell Physiol* 2013, **228**(7):1487-1495.
56. Kahraman M, Laufer T, Backes C, Schrors H, Fehlmann T, Ludwig N, Kohlhaas J, Meese E, Wehler T, Bals R *et al*: **Technical Stability and Biological Variability in MicroRNAs from Dried Blood Spots: A Lung Cancer Therapy-Monitoring Showcase**. *Clin Chem* 2017, **63**(9):1476-1488.
57. Slattery ML, Lee FY, Pellatt AJ, Mullany LE, Stevens JR, Samowitz WS, Wolff RK, Herrick JS: **Infrequently expressed miRNAs in colorectal cancer tissue and tumor molecular phenotype**. *Mod Pathol* 2018, **31**(1):209.
58. Huang X, Yuan T, Tschannen M, Sun Z, Jacob H, Du M, Liang M, Dittmar RL, Liu Y, Liang M *et al*: **Characterization of human plasma-derived exosomal RNAs by deep sequencing**. *BMC Genomics* 2013, **14**:319.
59. Wang L, Li Y, Guan X, Zhao J, Shen L, Liu J: **Exosomal double-stranded DNA as a biomarker for the diagnosis and preoperative assessment of pheochromocytoma and paraganglioma**. *Mol Cancer* 2018, **17**(1):128.
60. Kyuno D, Zhao K, Bauer N, Ryschich E, Zoller M: **Therapeutic Targeting Cancer-Initiating Cell Markers by Exosome miRNA: Efficacy and Functional Consequences Exemplified for claudin7 and EpCAM**. *Transl Oncol* 2019, **12**(2):191-199.
61. Manna I, Iaccino E, Dattilo V, Barone S, Vecchio E, Mimmi S, Filippelli E, Demonte G, Polidoro S, Granata A *et al*: **Exosome-associated miRNA profile as a prognostic tool for therapy response monitoring in multiple sclerosis patients**. *FASEB J* 2018, **32**(8):4241-4246.
62. Iliev D, Strandskog G, Nepal A, Aspar A, Olsen R, Jorgensen J, Wolfson D, Ahluwalia BS, Handzhiyski J, Mironova R: **Stimulation of exosome release by extracellular DNA is conserved across multiple cell types**. *FEBS J* 2018.
63. Smith RA, Lam AK: **Liquid Biopsy for Investigation of Cancer DNA in Esophageal Adenocarcinoma: Cell-Free Plasma DNA and Exosome-Associated DNA**. *Methods Mol Biol* 2018, **1756**:187-194.

Acknowledgments
We thank Dr. Qingfu Zhu for helping with the preparation of 3D cell culture and TEM imaging of 3D cultured cells. We also thank John Sibbitts for developing confocal imaging of 3D cells and developing exosomal RNA/DNA extraction protocols. We acknowledge the funding support from USDA-NIFA KS451214 and NIH NIGMS P20 GM103638. We also thank the assistant from Jennifer Hackett from the Genomic Core at the University of Kansas for library preparation, quality check and next-generation sequencing.

Author contributions statement
Miss Sirisha Thippabhotla drafted the manuscript, performed database searching, bioinformatics analysis and statistical data analysis, and draw the data figures. Miss Lanjing Wei performed the cell culture and exosome collection for RNAs and DNAs extraction. Dr. Cuncong Zhong performed overall data collection and analysis, as well as the manuscript revision. Dr. Mei He conceived the research idea, analyzed the data, and revised the manuscript.

Additional information
There is no conflict of interest to disclose